INSAR DEFORMATION TIME SERIES CLASSIFICATION USING A CONVOLUTIONAL NEURAL NETWORK

S.M. Mirmazloumi [1, *], Á.F. Gambin [2], Y. Wassie [1], A. Barra [1], R. Palamà [1],
M. Crosetto [1], O. Monserrat [1], B. Crippa [3]

[1] Centre Tecnològic de Telecomunicacions de Catalunya (CTTC/CERCA), Geomatics Research Unit, Av. Gauss, 7,
E-08860 Castelldefels (Barcelona), Spain - sm.mirmazloumi@cttc.es
[2] Artificial Intelligence Lab, Oslo Metropolitan University, Oslo, Norway - angelfer@oslomet.no
[3] Dept. of Geophysics, University of Milan, Via Cicognara 7, I-20129 Milan, Italy - bruno.crippa@unimi.it

KEY WORDS: SAR, CNN, Deformation Time Series, Persistent Scatterer Interferometry, Sentinel-1.

ABSTRACT:

Temporal analysis of deformations Time Series (TS) provides detailed information of various natural and humanmade displacements. Interferometric Synthetic Aperture Radar (InSAR) generates millimetre-scale products, indicating the chronicle behaviour of detected targets via TS products. Deep Learning (DL) can handle a massive load of InSAR TS to categorize significant movements from non-moving targets. To this end, we employed a supervised Convolutional Neural Network (CNN) model to distinguish five deformations trends, including Stable, Linear, Quadratic, Bilinear, and Phase Unwrapping Error (PUE). Considering several arguments in a CNN model, we trained numerous combinations to explore the most accurate combination from 5000 samples extracted from a Persistent Scatterer Interferometry (PSI) technique and Sentinel-1 images over the Granada region, Spain. The model overall accuracy exceeds 92%. Deformations of three cases of landslides were also detected over the same area, including the Cortijo de Lorenzo, El Arrecife, and Rules Viaduct areas.

1. INTRODUCTION

Ground deformations are physical events caused by natural or human activities, that can be analyzed to provide the status of natural and anthropic hazards. Remote sensing provides tools to investigate the temporal and spatial analysis of ground deformation. The extensive archive of Synthetic Aperture Radar (SAR) images, such as Sentinel-1, provides a rich data source for Interferometric SAR (InSAR) techniques, which can measure ground deformations at millimeter-scale. InSAR is generated from the interferometric phase of at least two SAR images for a certain area of interest (Crosetto et al., 2016; Minh et al., 2020). Advanced Differential InSAR (DInSAR) techniques, like Persistent Scatterer Interferometry (PSI) generate deformation Time Series (TS), which are extracted by multiple consecutive SAR acquisitions over the same area (Crosetto et al., 2016). This product offers deformations history over observed targets, which can recognize various types of natural hazards and artifacts (Crosetto et al., 2016; Minh et al., 2020).

Considering the availability of big InSAR datasets, data management tools are required to efficiently utilize them for long-term monitoring (Minh et al., 2020). The Deep Learning (DL) framework, the developed version of Neural Networks (NN), and more specifically Artificial Neural Networks (ANN), poses great opportunities regarding the management of large-size data to aid in earth environmental applications (Yuan et al., 2020). Convolution Neural Network (CNN) has been widely used in various remote sensing applications, including image classification, object detection, and targets recognition (Ma et al., 2019; Yuan et al., 2020; Zhu et al., 2017). Due to the robust functionality of CNN in the recognition task (Yuan et al., 2020), it has been recently proposed to investigate ground deformation using satellite images. For example, Mohan et al. (2021) reviewed the advantages of remote sensing data and machine learning techniques (e.g., DL) in landslide detection. Different

studies were also conducted on the CNN algorithm to improve the landslide susceptibility evaluation (Shibao and Jie, 2021), volcanic surface deformation (Sun et al., 2020), land subsidence (Radman et al., 2021; Shimosato and Ukita, 2021), and deformations of built regions (Anantrasirichai et al., 2021) using InSAR datasets.
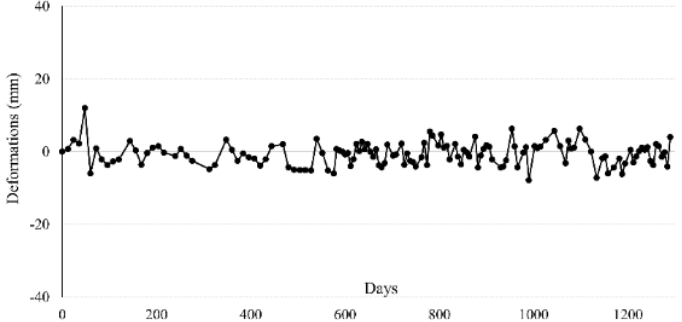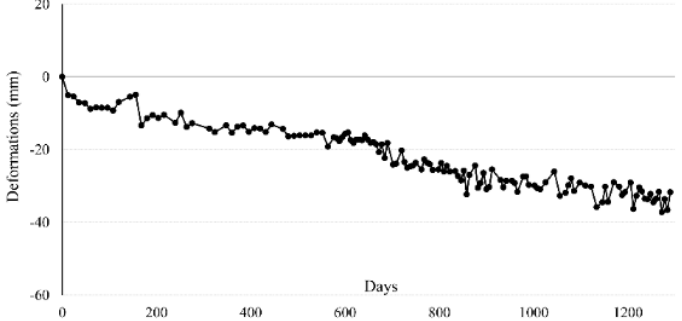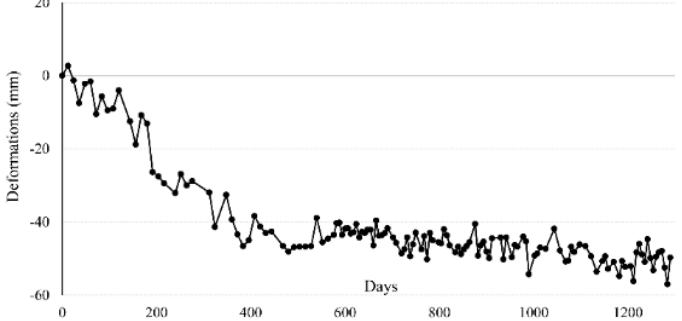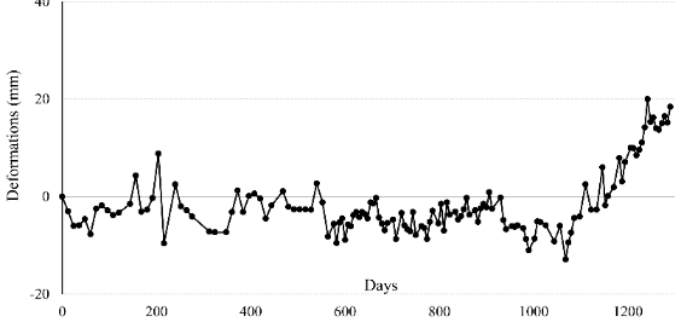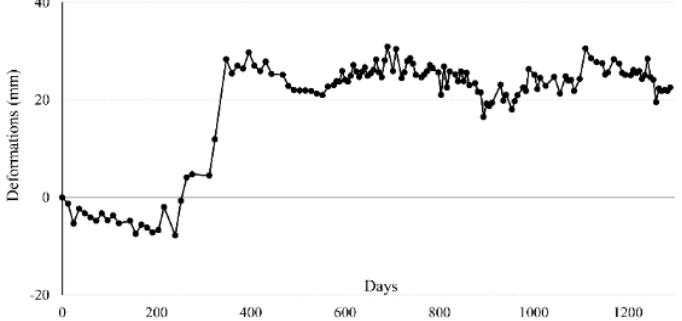
Classification of ground deformations TS to identify moving and non-moving targets can decrease the burden of big InSAR data analysis and provide detailed information of various natural and humanmade displacements. DL models can handle a massive load of InSAR TS to categorize the significant movements by deformations TS classification from non-moving targets. DL strategies also employ various frameworks to improve models for the most accurate outcomes, such as CNN. In this paper, we train a supervised CNN model to distinguish five deformations trends, including Stable, Linear, Quadratic, Bilinear, and Phase Unwrapping Error (PUE) using 5000 labeled samples of Granada dataset. Additionally, the proposed model is employed to identify ground motions over three cases of landslides in Granada, Spain. These trends were so far proposed as the dominant types of deformations TS by Berti et al. (2013).

The remainder of the paper is structured as follows: Section 2 describes the dataset and study areas and defines five deformation classes. Section 3 presents the proposed methodology, architecture of the CNN model, and accuracy assessment procedure. In Section 4, we examined the proposed methodology and discussed the obtained results. Finally, main conclusions are presented in Section 5.

2. STUDY AREA AND DATA

In this section, first the study area is described, then the characteristics of the DInSAR dataset is provided. Additionally, five deformation trends are explained by visual examples.

---

* Corresponding author

Class	Trend	Description
Stable		No deformation occurs. The TS consists of small random variations.
Linear		A constant slope characterizes TS.
Quadratic		The displacements follow a quadratic law and a continuous movement.
Bilinear		TS is divided by a breakpoint into two segments with different linear rates.
PUE		There could be one or more jumps due to phase unwrapping errors inside one TS.

Table 1. Descriptions and visual examples of five deformation classes based on definitions provided by (Berti et al., 2013; Mirmazloumi et al., 2022).

2.1 Study area

The Rules Reservoir is located in Granada, southern Spain, where collects water from the south and western regions. In addition to Rules Dam, there are two important transport infrastructures in this region, affected by three landslides (Reyes-Carmona et al., 2020): Cortijo de Lorenzo area (A), the El Arrecife Landslide (B), and the Rules Viaduct Landslide (C) (see Figure 2).

2.2 Dataset and Reference Samples

To analyze the unstable areas of Rules Reservoir region, 139 Sentinel-1A and Sentinel-1B images from March 2015 to September 2018 were processed through the PSI chain of the Geomatics Division (PSIG) of the Centre Tecnològic de Telecomunicacions de Catalunya (CTTC) (Devanthéry et al., 2014). The estimated deformation TSs are along the satellite Line of Sight (LoS) direction. In this study, we utilize the deformation TS product of the study area to classify stable and unstable targets focusing on the temporal behavior of ground motions.

Deformation TS are categorized into two types of movements: stable and unstable. Stable TSs indicate small and random fluctuations, containing areas without significant movements. On the other hand, unstable TSs can be expanded to various trends based on velocities of deformations and changes in velocities. Berti et al. (2013) comprehensively described different deformations TSs in seven trends. This study proposes five deformations trends as labeled samples to train and test the proposed model. The description and visual example of all five classes are provided in Table 1. One thousand samples per class were selected from the InSAR TS of Granada dataset as reference samples to classify deformations of the study areas.

3. METHODOLOGY

DL is a potential tool for conducting complex tasks due to its demonstrated skill to approximate the complicated nonlinear relationship between various environmental variables, multi-layer learning, multiscale and multilevel feature extracting, and outperforming traditional methods with advanced analysis (Yuan et al., 2020). CNNs are feed-forward deep neural networks comprising a series of convolutional layers between the input and output layers (Trinh et al., 2021). The convolutional layers include kernels, pooling, and activation units. Each kernel consists of a number of weights convolving across the input dataset to enhance the network's connectivity and reduce computational complexity. Additionally, the pooling layers (e.g., max and average pooling) operate the input data dimensions reduction toward the next layers. Activation layers (or functions) increase the capability of non-linear fitting of CNN models.

Figure 1 shows the proposed CNN architecture that we designed to classify deformation TSs. Initially, the representation of input samples is changed to a machine learning-based data preparation, one-hot encoding, to avoid poor performance of DL models and unexpected results. This encoding changes the natural ordered form of categorical data to improve prediction accuracy (Brownlee, 2020).

After the input data preparation, the first convolutional layer, Conv_1, uses 138 kernels with 5 sample sizes to filter and process input TSs using the ReLU activation function. The second block, Conv_2, also includes similar characteristics using 64 kernels. Max pooling is separately applied to the outputs of Conv_1 and _2 with kernel sizes of 2 to decrease their dimensionality. In the fully connected Conv_3 layer, an average pooling is implemented to the convolutional layer with a 0.4 dropout rate to control the overfitting. In the last layer, a Leaky ReLU activation function is applied to the fully connected layer to reduce the computation time. Afterward, the classes probabilities are estimated by the softmax activation function to assign the most probable label to training datasets. In this study, 5000 reference samples are divided into training, validation, and testing sets with a split ratio of 70% - 10% - 20%.

The classification performance is assessed by the following metrics:

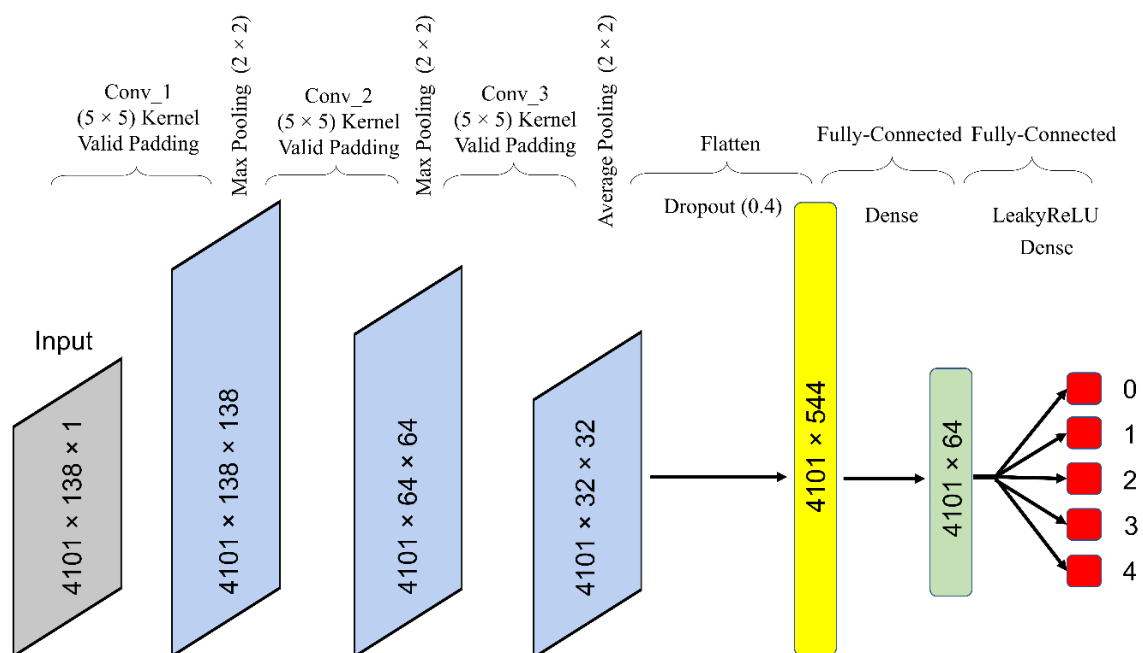1- Confusion matrix: includes the number of correctly classified to the total number of samples in each class.

Figure 1. The proposed CNN architecture proposed in this study.

2- Precision: the ratio between true positives T_p and the sum of true positives with false positives F_p:

$$P = \frac{T_p}{T_p + F_p} \qquad (1)$$

3- Recall: the ratio of T_p to the sum between T_p and F_n:

$$R = \frac{T_p}{T_p + F_n} \qquad (2)$$

4- F-Score: measures the harmonic mean of precision and recall:
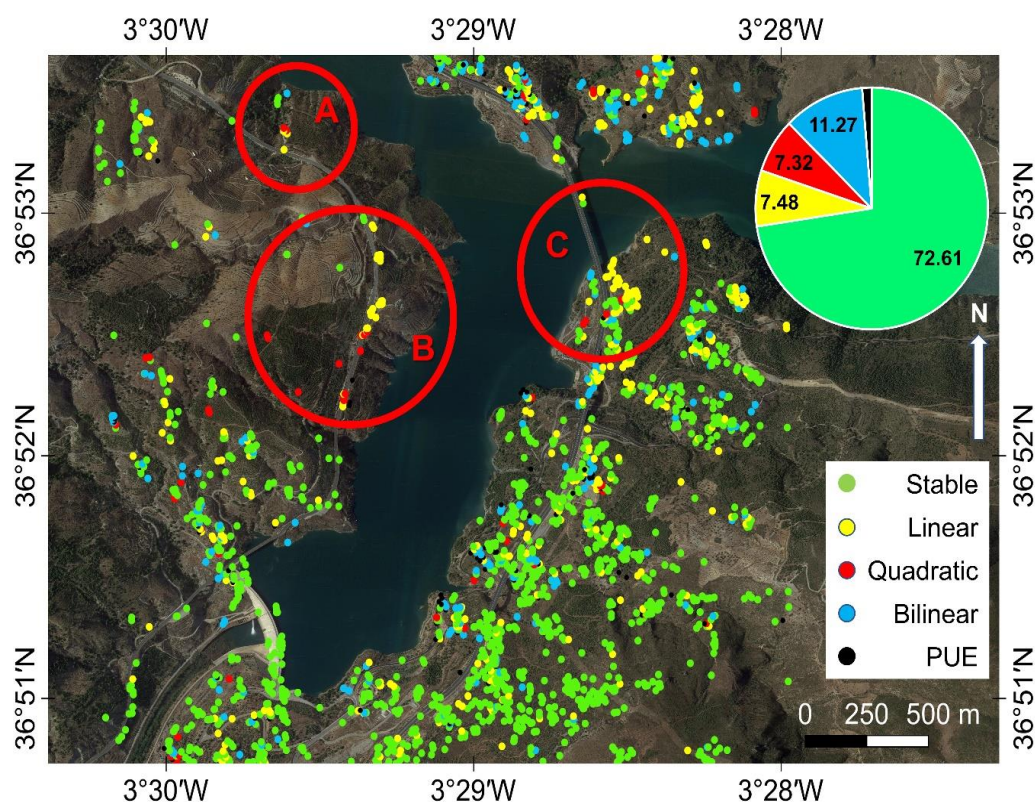
$$F - Score = 2\frac{RP}{R + P} \qquad (3)$$

4. RESULTS

The methodology was implemented in Python using *tensorflow* (*keras* framework) and *sklearn* libraries. The method was also carried out using an Intel Core i7 machine with 32 GB of RAM and an Intel UHD Graphics 630 GPU card.

Figure 2 shows the classified map of the Rules Reservoir by the CNN model in five deformation trends. The area includes three landslides, where most unstable trends (e.g., Linear, Quadratic, and Bilinear) occur. The figure also indicates the capability of the CNN model in identifying ground motions over unstable areas.

Three landslides include the Cortijo de Lorenzo area (A), the El Arrecife Landslide (B), and the Rules Viaduct Landslide (C). The dominant number of targets (approximately 73%) were classified as Stable points. However, several unstable classes were detected over three landslides, of which around 26% of targets were identified as unstable targets (i.e., Linear, Quadratic, and Bilinear) among 4459 points measured in this area. Furthermore, 56 points with PU errors were classified by the CNN model. Moreover, most deformations were found in western regions of the study area, located close to a national road and within the El Arrecife Landslide, including Linear and Quadratic TSs. A set of Linear and Quadratic targets were also detected nearby a highway in the east, called the Rules Viaduct Landslide. Additionally, several Bilinear deformations occurred in the Cortijo de Lorenzo area, where the displacements were less significant than in other regions. Moreover, a few unstable targets were found in the north of this region, indicating instabilities due to the unstable slopes.

Table 2 summarizes the performance of CNN in the classification of test datasets. The overall accuracy was derived 92.30%, indicating the proposed model reasonable capability in identifying deformation TS. The estimated values in Table 2 also show that the classifier performed efficiently for categorizing all classes. The most precise classification was reported in the Stable class, which was expected due to the uncomplex behavior of this trend. Although the precision of the PUE class was 0.95, the estimated recall (0.76) and F-Score (0.84) values demonstrated that the model was not able to classify this class as accurate as other classes. Furthermore, the proposed model was able to identify unstable classes with more than 0.85 in all metrics, showing an accurate tool to detect ground movements.

Figure 2. Ground deformation TS classified map of the Rules Reservoir, including Cortijo de Lorenzo area (A), the El Arrecife Landslide (B), and the Rules Viaduct Landslide (C) in red circles. The pie chart shows the portion of each deformation trend over the study area.

Class	P	R	F1-Score	
Stable	0.97	0.96	0.97	
Linear	0.89	0.99	0.94	
Quadratic	0.86	0.91	0.88	
Bilinear	0.96	0.97	0.96	
PUE	0.95	0.76	0.84	
			OA	92.30%

Table 2. The CNN classifier performance.

The confusion matrix of the proposed CNN architecture is shown in Figure 3, preparing a deeper look at the model performance. The rows and columns present true and predicted samples, respectively, whereas 0 to 4 are the predicted classes. Except in the PUE class, a few samples were confused (i.e., misclassified) with other classes. Approximately 24% of the PUE class was confused by other trends, while the confusion rate of the rest of the classes was less than 9%. It is worth mentioning that the amount of noise highly affects the vertical jumps in PUE, which can cause misclassification of this trend. Furthermore, the PUE class is categorized as a non-linear trend, similar to Quadratic and Bilinear, where most confusions occurred. Among unstable classes, the most misclassification rates were founded between Quadratic and Linear classes (7.11%), which can be those quadratic TSs with lower curvatures.

Figure 3. The confusion matrix of the proposed CNN. The predicted numbers stand as Stable:0, Linear:1, Quadratic:2, Bilinear:3, and PUE:4.

5. CONCLUSION

In this work, we tailored a supervised CNN model to classify five deformation trends over a study area in Granada, Spain. The CNN model was selected due to DL ability to handle big data and accurate performance. Deformation TSs were provided by the PSIG technique from 139 Sentinel-1 images, and 5000 samples were labeled among the measured points. The proposed architecture was able to classify labeled deformation TS with 92.30% accuracy and reasonable values of other performance metrics for each class. The proposed CNN was also applied over a region including three landslides to detect moving TSs

characterized by unstable trends. Around 1170 unstable points were classified as moving targets, where the dominant number was found over landslides. Finally, it is worth mentioning that DL algorithms can provide valuable tools to conventional InSAR techniques for ground motion monitoring. We showed the ability of the CNN model in the accurate classification of moving and non-moving targets. As a future research direction, the efficiency of DL frameworks in big InSAR data can be addressed by adopting DL models on large-scale regions and numerous SAR images.

REFERENCES

Anantrasirichai, N., Biggs, J., Kelevitz, K., Sadeghi, Z., Wright, T., Thompson, J., Achim, A.M., Bull, D., 2021. Detecting Ground Deformation in the Built Environment Using Sparse Satellite InSAR Data with a Convolutional Neural Network. IEEE Trans. Geosci. Remote Sens. 59, 2940–2950. https://doi.org/10.1109/TGRS.2020.3018315

Berti, M., Corsini, A., Franceschini, S., Iannacone, J.P., 2013. Automated classification of Persistent Scatterers Interferometry time series. Nat. Hazards Earth Syst. Sci. 13, 1945–1958. https://doi.org/10.5194/nhess-13-1945-2013

Brownlee, J., 2020. Machine Learning Mastery With Python: Data Cleaning, Feature Selection, and Data Transforms in Python.

Crosetto, M., Monserrat, O., Cuevas-González, M., Devanthéry, N., Crippa, B., 2016. Persistent Scatterer Interferometry: A review. ISPRS J. Photogramm. Remote Sens. https://doi.org/10.1016/j.isprsjprs.2015.10.011

Devanthéry, N., Crosetto, M., Monserrat, O., Cuevas-González, M., Crippa, B., 2014. An approach to persistent scatterer interferometry. Remote Sens. 6, 6662–6679. https://doi.org/10.3390/rs6076662

Ma, L., Liu, Y., Zhang, X., Ye, Y., Yin, G., Johnson, B.A., 2019. Deep learning in remote sensing applications: A meta-analysis and review. ISPRS J. Photogramm. Remote Sens. https://doi.org/10.1016/j.isprsjprs.2019.04.015

Minh, D.H.T., Hanssen, R., Rocca, F., 2020. Radar interferometry: 20 years of development in time series techniques and future perspectives. Remote Sens. 12. https://doi.org/10.3390/RS12091364

Mirmazloumi, S.M., Wassie, Y., Navarro, J.A., Palamà, R., Krishnakumar, V., Barra, A., Cuevas-González, M., Crosetto, M., Monserrat, O., 2022. Classification of ground deformation using sentinel-1 persistent scatterer interferometry time series. GIScience Remote Sens. 59, 374–392. https://doi.org/10.1080/15481603.2022.2030535

Mohan, A., Singh, A.K., Kumar, B., Dwivedi, R., 2021. Review on remote sensing methods for landslide detection using machine and deep learning. Trans. Emerg. Telecommun. Technol. 32. https://doi.org/10.1002/ett.3998

Radman, A., Akhoondzadeh, M., Hosseiny, B., 2021. Integrating InSAR and deep-learning for modeling and predicting subsidence over the adjacent area of Lake Urmia, Iran. GIScience Remote Sens. 58, 1413–1433. https://doi.org/10.1080/15481603.2021.1991689

Reyes-Carmona, C., Barra, A., Galve, J.P., Monserrat, O., Pérez-Peña, J.V., Mateos, R.M., Notti, D., Ruano, P., Millares, A., López-Vinielles, J., Azañón, J.M., 2020. Sentinel-1 DInSAR for monitoring active landslides in critical infrastructures: The case of the rules reservoir (Southern Spain). Remote Sens. 12. https://doi.org/10.3390/rs12050809

Shibao, W., Jie, W., 2021. Evaluation of Landslide Susceptibility of the Ya ' an- Linzhi Section of the Sichuan-Tibet Railway based on Deep Learning. https://doi.org/10.21203/rs.3.rs-714294/v2

Shimosato, K., Ukita, N., 2021. Multi-Modal Data Fusion for Land-Subsidence Image Improvement in PSInSAR Analysis. IEEE Access 9, 141970–141980. https://doi.org/10.1109/ACCESS.2021.3120133

Sun, J., Wauthier, C., Stephens, K., Gervais, M., Cervone, G., La Femina, P., Higgins, M., 2020. Automatic Detection of Volcanic Surface Deformation Using Deep Learning. J. Geophys. Res. Solid Earth 125. https://doi.org/10.1029/2020JB019840

Trinh, H.D., Fernandez Gambin, A., Giupponi, L., Rossi, M., Dini, P., 2021. Mobile Traffic Classification through Physical Control Channel Fingerprinting: A Deep Learning Approach. IEEE Trans. Netw. Serv. Manag. 18, 1946–1961. https://doi.org/10.1109/TNSM.2020.3028197

Yuan, Q., Shen, H., Li, T., Li, Z., Li, S., Jiang, Y., Xu, H., Tan, W., Yang, Q., Wang, J., Gao, J., Zhang, L., 2020. Deep learning in environmental remote sensing: Achievements and challenges. Remote Sens. Environ. 241. https://doi.org/10.1016/j.rse.2020.111716

Zhu, X.X., Tuia, D., Mou, L., Xia, G.S., Zhang, L., Xu, F., Fraundorfer, F., 2017. Deep Learning in Remote Sensing: A Comprehensive Review and List of Resources. IEEE Geosci. Remote Sens. Mag. https://doi.org/10.1109/MGRS.2017.2762307